

PHYSICS PROBLEMS OF THERMONUCLEAR REACTORS*

F. L. Ribe

University of California, Los Alamos Scientific Laboratory
Los Alamos, New Mexico 87544

ABSTRACT

A problem common to all controlled fusion reactors is that of the burning deuterium-tritium fuel under conditions of plasma confinement which approach the ideal limit as nearly as possible. After ignition, the balance between alpha-particle energy deposition and plasma losses (radiation plus thermal and particle diffusion) determines the stability or instability of the burn in toroidal systems. Tokamak systems are described both with unstable, injection-regulated burn cycles and stabilized steady-state burn conditions. In the theta-pinch reactor an unstable burn occurs, somewhat regulated by high-beta plasma expansion, which is quenched by a programmed plasma decompression. The plasma expansion during the constant-pressure burn provides "direct" conversion of plasma thermonuclear heat to electrical output, in addition to the electrical power derived from the neutron energy through conventional thermal conversion equipment. The open-ended mirror reactor is characterized by a direct conversion system for recovering end-loss plasma energy and converting it to electrical energy for reinjection into the plasma. This allows a favorable reactor energy balance an an amplification factor Q (= thermonuclear energy output/injected plasma energy) which is compatible with classical collisional losses. For the three reactor types considered the ramifications of burn and confinement conditions for reactor configuration, energy balance, economy, fuel handling, materials problems, and environmental-radiological factors are considered.

I. INTRODUCTION

The preceding paper by H. P. Furth¹ describes the basic concepts of thermonuclear processes and magnetic confinement in fusion reactors and gives a brief summary of the present state of research on the major experiments. In the present paper a brief description will be given of the properties of conceptual reactor systems based on the three major magnetic confinement systems presently being investigated. Conceptual fusion reactor studies have been pursued since 1965, and a summary of the early work is to be found in the proceedings of the 1969 Culham Conference on Nuclear Fusion Reactors.² The conceptual designs which are summarized here stem from the following more recent detailed work over the last two or three years: (a) three Tokamak reactor studies at the Princeton Plasma Physics Laboratory (PPPL)³, the Oak Ridge

* Work performed under the auspices of the U. S. Atomic Energy Commission.

MASTER

National Laboratory (ORNL),^{4,5} and the University of Wisconsin (UWMAK design)⁶, (b) a Theta-Pinch reactor study carried out jointly by the Los Alamos Scientific Laboratory (LASL) and the Argonne National Laboratory (ANL)⁷; and (c) a Magnetic-Mirror reactor study at the Lawrence Livermore Laboratory (LLL).⁸ In all of these studies plasma heating and confinement are assumed to occur according to idealized physical laws, to degrees not yet attained in the experiments, and the emphasis is on the physical problems imposed by the engineering demands of the thermal and nuclear environment and the requirements of practical power generation. The power levels and dimensions of the reactors represent compromises between economically desirable high power densities and the low power densities, and large sizes which alleviate materials problems.

II. FUSION-REACTOR CONFIGURATIONS AND POWER BALANCE

In this review we consider only the D-T fusion reaction (Table I, Reference 1) as a basis for reactor design, since its peak cross section occurs at relatively low ion temperature, allowing reactor operation at 100 to 200×10^6 °C (11.4 to 22.8 keV) in closed systems and 4 to 6×10^7 °C (45.6 to 68.4 keV) in magnetic-mirror systems. Because of this it is expected that the D-T reaction will be the basis of first-generation fusion reactors. Later power plants will probably make use of the D-D and D-He³ reactions in which the absence of 14-MeV neutrons and their interaction with the reactor structure will be an advantage, gained at the cost of much higher plasma temperatures.

Figure 1 is a generalized cross section of the core of a magnetic

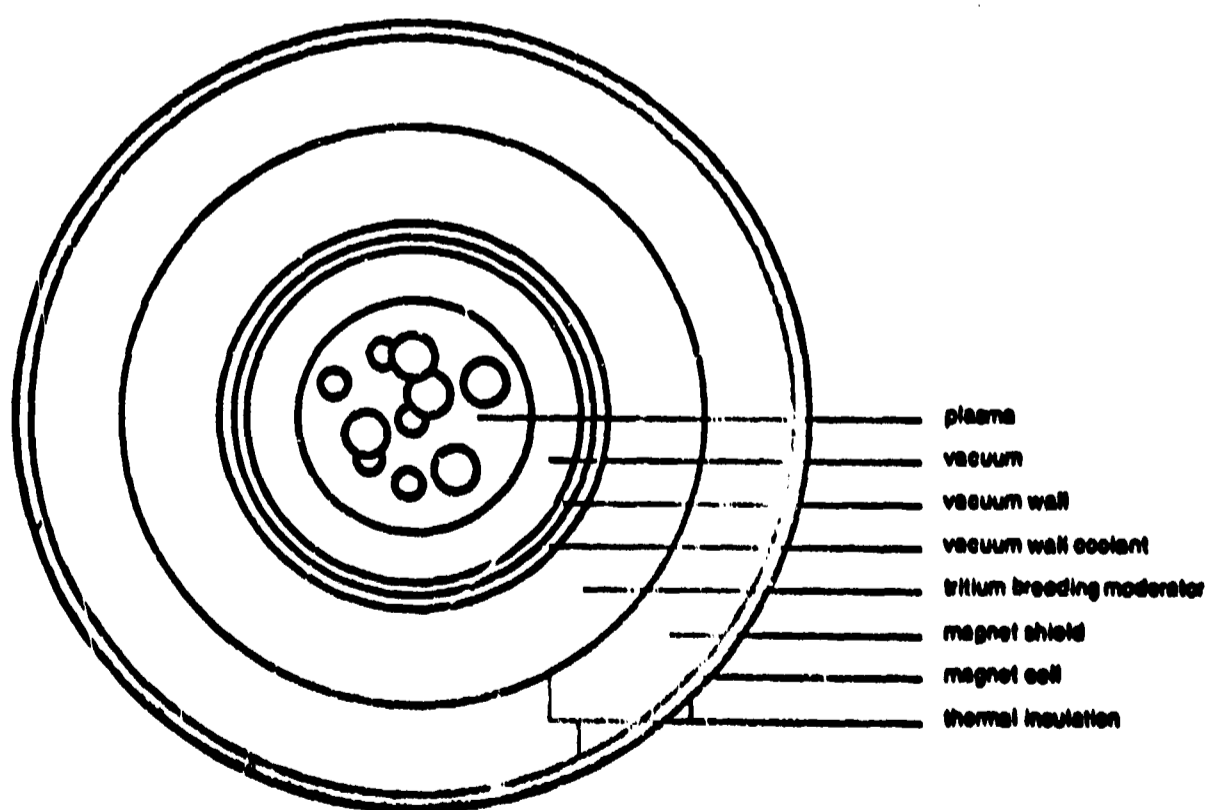


Fig. 1. Generalized cross section of the core of a nuclear fusion reactor.

confinement fusion reactor. The plasma is confined by magnetic fields (predominantly perpendicular to the plane of the figure) in excess of 6 T. Plasma ion and electron densities are in the range of 10^{20} m^{-3} for Tokamak and Mirror reactors and 10^{22} m^{-3} for the Theta-Pinch reactor. The magnetic coil producing the magnetic field is protected from the nuclear radiation of the plasma by means of a moderator and absorber of the neutrons and gamma rays, a magnet shield which absorbs neutrons and gamma rays, and thermal insulation. In the case of a deuterium-tritium plasma the moderator may breed tritium to replace that depleted from the plasma as fusion reactions take place. The plasma is surrounded by vacuum or low-density plasma, the whole being contained in a vacuum vessel with a first wall as shown. A coolant, consisting of flowing liquid metal, salt or high-pressure gas, removes heat deposited in the vacuum wall by nuclear and electromagnetic radiation from the plasma.

A quantity of basic importance to fusion physics and reactor design is the ratio β of the kinetic pressure $p = 2nkT$ of the plasma ions and electrons to the pressure of the external confining magnetic field B perpendicular to the plane of Fig. 1:

$$\beta = p/(B^2/2\mu_0) = 4\mu_0 nkT/B^2. \quad (1)$$

In present experiments "low" beta refers to values less than 0.01 and "high" beta values lie between 0.1 and 1.0 (the maximum possible).

A quantity basic to the plasma dynamics is the reaction-rate parameter which is the product $\langle\sigma v\rangle$ of the D-T reaction cross section and relative D-T velocity, averaged over a Maxwellian velocity distribution. If we assume equal number densities n of deuterons and tritons the thermonuclear power available for each m^3 of plasma for thermal conversion to electricity or some other form of work is

$$P_T = \frac{1}{4} n^2 \langle\sigma v\rangle Q \quad (2)$$

where $Q = ME_n + E_\alpha$, and E_n and E_α are the neutron and α -particle energies of Table I, Ref. 1. The quantity M is the energy produced in the moderating blanket by each 14-MeV neutron. Substituting n from (2) we find

$$P_T = 0.78 \times 10^{23} \beta^2 B^4 Q \langle\sigma v\rangle / T^2, \quad (\text{W/m}^3) \quad (3)$$

where Q and T are in eV. The dependence on β^2 shows the importance of the quantity beta as a measure of utilization of magnetic-field energy in fusion reactors.

The heating of the plasma is derived from the α particles which remain in the plasma, depositing a power density

$$P_\alpha = \frac{1}{4} n^2 \langle\sigma v\rangle E_\alpha = 5.1 \times 10^{-29} n^2 \frac{\exp(-200/T_i^{1/3})}{T_i^{2/3}}, \quad (\text{W/m}^3) \quad (4)$$

where T_e (in eV) is the (assumed) common temperature of the deuterons and tritons, each of which is assumed to have number density $n(m^{-3})$.

The Bremsstrahlung power density for the range of n and T values appropriate to D-T reactors is given by

$$p_{Br} = 1.7 \times 10^{-38} n^2 Z^2 T_e^{1/2}, \quad (W/m^3) \quad (5)$$

where Z is the ionic charge, and n is the electron density in m^{-3} . This represents the total emission of all wavelengths of the continuum from the (optically thin) plasma (T_e in eV). In addition there is a plasma loss p_s from the synchrotron radiation emitted by the electrons in their magnetic orbits which occurs at low β , low n and high T , as well as a heat-loss power density P_Q arising from radial particle diffusion and heat conduction. This heat loss is usually characterized by an energy-loss e-folding time τ_E :

$$P_Q = 3\pi a^2 nT/\tau_E, \quad (6)$$

where a is the plasma radius. Another important means of raising the energy of a plasma is adiabatic compression whereby a rate of increase \dot{B} of magnetic field causes the density and temperature to rise. Assuming the plasma to be a perfect gas characterized by a specific heat ratio γ , the rate of increase of internal energy density is given by

$$P_C = 3(\gamma - 1) B\dot{B}/\mu_0. \quad (7)$$

Finally, it is convenient to define a power deposition by injected beams of neutral atoms, each of energy E_0 :

$$P_I = SE_0. \quad (8)$$

In case of D-T pellet injection $E_0 \approx 0$, while for energetic ions deuterium and tritium ions E_0 is in the range of 500 keV.

As an example of plasma power-balance in a low-beta reactor (where β is assumed constant) consider the Tokamak case illustrated in Fig. 2. The ohmic heating rapidly declines with rising temperature and becomes ineffective in the temperature range of a few keV. The α -particle heating, on the other hand, rises rapidly in this temperature region. At the highest temperatures achieved by ohmic heating, the sum of ohmic and α -particle heating is not sufficient to overcome the losses due to ion heat conduction and Bremsstrahlung. Thus the plasma cannot get into the "ignited" regime $T \gtrsim 4$ keV where α -particle heating alone exceeds the losses and the plasma would become thermally self-sustaining. In order to achieve ignition an additional heat source of ~ 20 MW is necessary to bridge the gap between the minimum of the heat input curve and the rising curve of total heat loss. At this writing, the favored means of supplying this loss is by neutral-beam injection.

The time dependence of plasma temperature is determined by the various power input and loss quantities discussed above. Neglecting synchrotron radiation and plasma injection the rate of change of plasma internal energy is

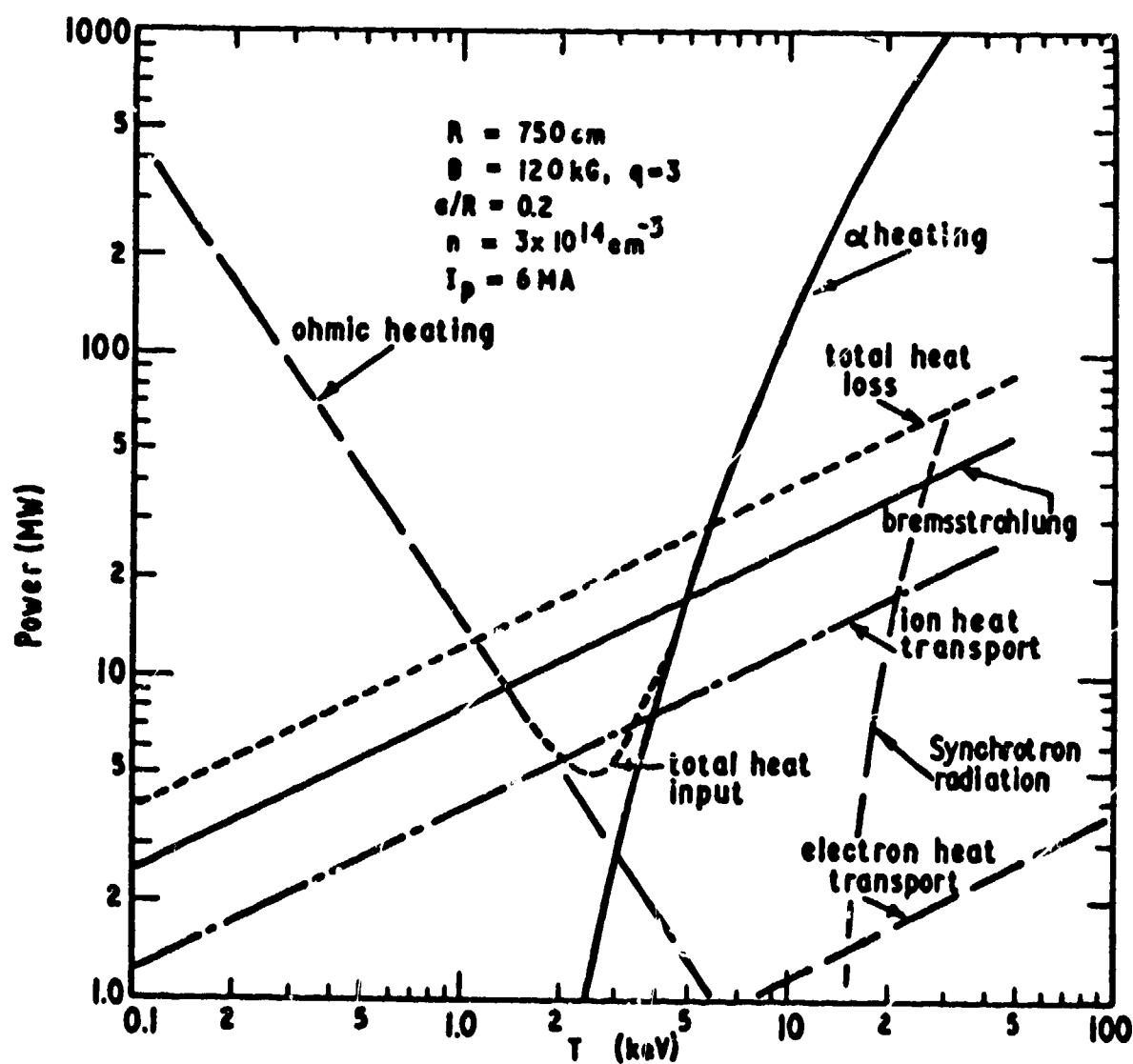


Fig. 2. Plasma power balance for a low-beta (Tokamak) reactor.⁹

$$d(3nT)dt = P_{\alpha} - P_{Br} - P_Q \quad (9)$$

Neglecting particle loss, as in a low- β reactor with small fuel burn-up, we find

$$dT/dt = nf(T) - T/\tau_E, \quad (10)$$

where $f(T) = (1/12) \langle \sigma v \rangle E_{\alpha} = 0.5 \times 10^{-38} T^{1/2}$. The condition for burning equilibrium $dT/dt = 0$ at same density n_0 and temperature T_0 is thus

$$n_0 \tau_E = T_0 / f(T_0). \quad (11)$$

It is easily shown, because of the rapid variation of $\langle \sigma v \rangle$ with T , that for τ_E 's which depend only weakly on T , this equilibrium is unstable. If τ_E is adjusted for a given T_0 small changes will cause an excursion of temperature upward toward the region of the $\langle \sigma v \rangle$ curve where the derivative is zero, or the temperature may decay, and the

reactor "goes out". At the unstable operating point it may be necessary to apply feedback control to the quantity τ_E or to $\langle \sigma v \rangle$.

The " $n\tau$ " condition (11) is superficially similar to the famous Lawson criterion which gives the condition that the electrical-energy output of a given plasma volume exceed the minimum energy $3 nT + P_{Br} \tau$ necessary to produce the plasma and hold it for time τ . However, the significances of the two conditions are greatly different. As an example, at $T = 20$ keV $n\tau_E$ is about 2×10^{20} sec/m³ and $n\tau$ (Lawson) is about 5×10^{19} sec/m³ for a 50%-50% D-T plasma.¹⁰

A quantity basic to the operation of a fusion reactor is the ratio Q of the thermonuclear power output P_T , from the plasma core to the thermal-conversion (turbine) equipment, to the injected power P_I necessary to sustain the plasma in a thermonuclear state:

$$Q = P_T / P_I. \quad (12)$$

The electrical power output of the thermal converter is

$$P_E = \eta_T P_T, \quad (13)$$

where η_T , related to the Carnot efficiency, is the efficiency at which heat is converted to output electrical power P_E in the thermal converter. Its values range from 0.35 to at most about 0.6. In order to provide the injection energy at some efficiency η_I a fraction ϵ of the plant electrical output P_E must be "recirculated". The circulating power fraction

$$\epsilon = P_I / \eta_I P_E = 1 / \eta_I \eta_T Q \quad (14)$$

is important as a cost determining factor, since it adds to the required capacity of the thermal conversion equipment. The fusion plant output power

$$P_P = (1 - \epsilon) P_E = \eta_P P_T \quad (15)$$

is related to the thermal power P_T of the reactor core by the plant efficiency

$$\eta_P = (1 - \epsilon) \eta_T. \quad (16)$$

III. TOKAMAK REACTORS

The essential features of a Tokamak diffuse toroidal pinch are shown in Fig. 4 of Ref. 1 and described in the Section III of that paper. It is useful to identify the poloidal beta β_θ , which is defined analogously to the axial or toroidal beta of Eq. (1). Thus

$$\beta_\theta = p / (B^2 / 2\mu_0) \quad (17)$$

where a is the minor plasma radius. The aspect ratio $A = R/a$, where R is the major radius. The ratio of the pitch length of the helical magnetic lines at the surface of the plasma to the major circumference $2\pi R$ is the so-called stability margin or safety factor

$$q = aB_{\phi}/RB_{\theta} = B_{\phi}/AB_{\theta}. \quad (18)$$

The beta quantity most often referred to, which enters the thermonuclear power density (3), is the toroidal beta

$$\beta_{\phi} = p/(B_{\phi}^2/2\mu_0) = \beta_{\theta}/(qA)^2. \quad (19)$$

In two of the designs to be discussed divertors form an important part of the reactor core. The basic object of a divertor is to prevent particles diffusing out of the plasma from hitting the first wall and to provide a means for removing α -particle "ash" and impurities while maintaining a steady through-put of fuel from injectors. If in addition the divertor zone has low neutral-gas pressure, it is a thermally insulating layer at the edge of the hot plasma, imposing the boundary condition $dT/dr = 0$ and hence a flat temperature distribution radially across the plasma.

The magnetic divertors considered here are based on the idea of generating a null in the poloidal (r, θ) field as shown in Fig. 3. This generates a separatrix outside of which field lines are carried away from the plasma as they pass the neutral points shown in Fig. 3 as the crossing points of the zero-field lines (separatrices). Inside a separatrix the magnetic flux surfaces remain closed, and the separatrix, rather than a material wall, is the effective boundary of the plasma.

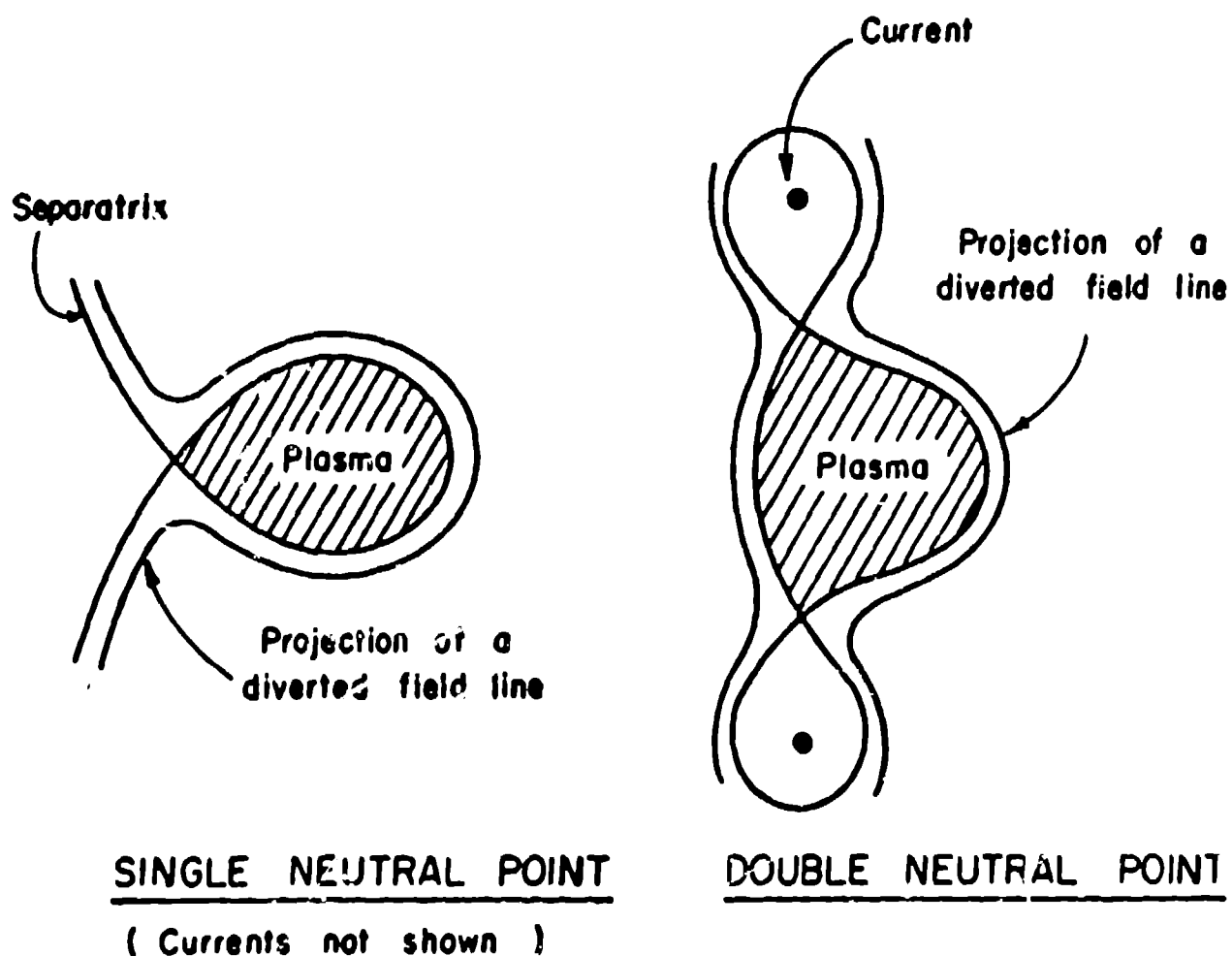


Fig. 3. Magnetic field configurations of poloidal field divertors.

Plasma particles diffuse across the separatrix and then follow the open field lines to particle collectors. The Tokamak design of the Princeton Group (Fig. 4) uses the single neutral-point divertor, while that of the University of Wisconsin group (Fig. 5) uses the double neutral point. The ORNL reactor (Fig. 6) has no divertor and uses a power cycle in which joule heating and neutral-beam injection produce ignition and peak power density. The plasma power density then subsides to a lower level which is sustained by the injectors. The UWMAK design (Fig. 5) operates in the unstable steady state, but in pulses whose length is determined by the decay of the poloidal field and the necessity to dispose of impurities not removed by the divertor. It uses joule heating and neutral beam injection, followed by D-T pellet injection. The PPPL design (Fig. 4) is conceived as a long-pulse, essentially steady-state system, fueled by D-T pellets.

Table I gives a comparison of the plasma and magnetic field parameters of the three conceptual Tokamak reactors. Note the large values of toroidal current (15-20 MA) and toroidal magnetic energy (100-300 GJ). In the UWMAK case the poloidal energy of 52 GJ would require a local superconducting magnetic-energy store (somewhat similar to that of a theta-pinch reactor) if the risetime of B_θ were of the order of 10 seconds or less, while for times of the order of 100 seconds the power to build up the poloidal energy [$\sim 500 \text{ MW(E)}$] could be taken "off the line". The

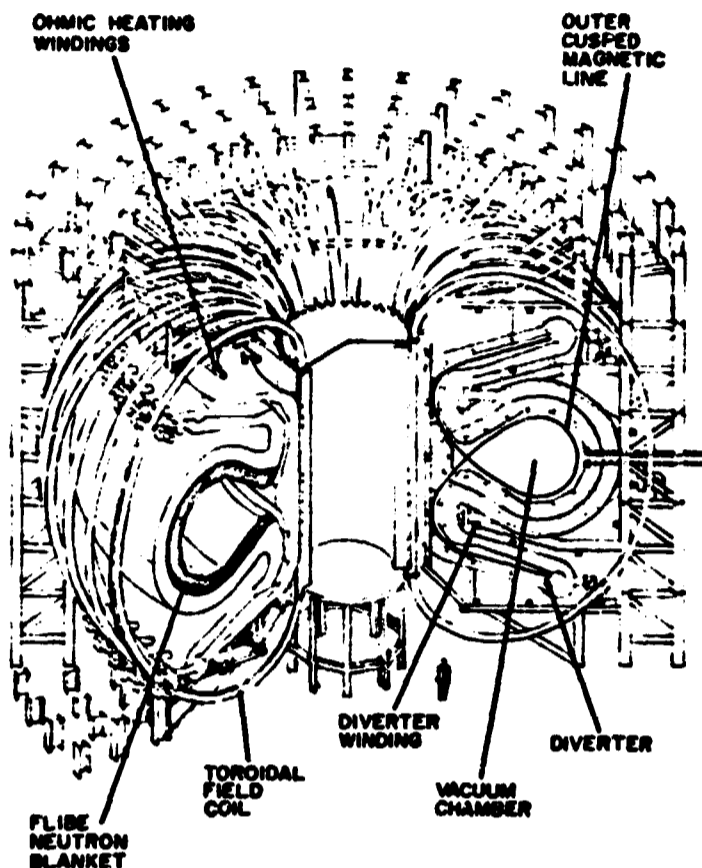


Fig. 4. PPPL Tokamak reactor.

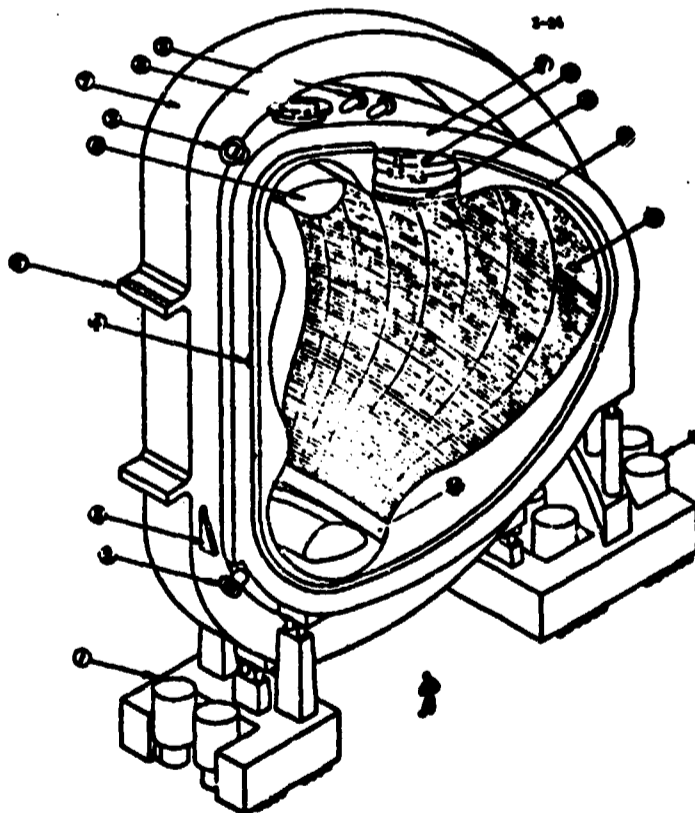
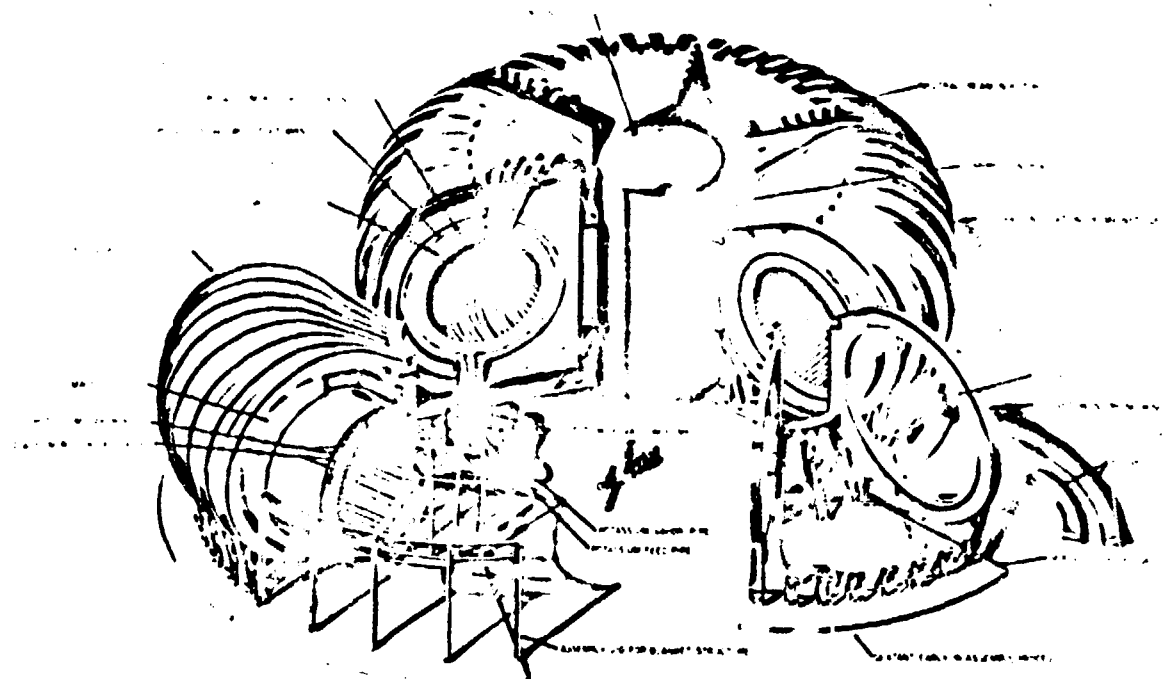


Fig. 5. UWMAK Tokamak reactor module.



TOROIDAL FUSION REACTOR (1000 MW)

Fig. 6. General view of the ORNL conceptual Tokamak reactor.

TABLE I Plasma and magnetic field parameters of the three conceptual Tokamak reactors

	ORNL	PPPL	UWMAK
Plasma:			
Poloidal Beta β_θ (Av.)	3.0	2.3	1.08
Toroidal Beta β_ϕ	0.15	0.11	0.052
Major Radius R, m	10.5	10.5	13
Minor Radius a, m	3.3	3.3	5
Aspect Ratio A	3.2	3.2	2.6
Safety Factor q	1.4	2.1	1.75
Magnetic Fields:			
Av, Tor, B_ϕ , kG	60	60	38
Max, Tor, B_ϕ , kG	147	160	87
Pol. Field B_θ (a), kG	13	9	8.4
Plasma Current MA	21	15	21
Tor. Mag. En. GJ	120	223	290
Pol. Mag. En. GJ	~10	-	52

superconducting UWMAK magnets (poloidal and toroidal) are Cu-stabilized NbTi (4°K), while the PPPL design uses Nb₃Sn (~12°K).

In respect to the first-wall, neutron-blanket and fueling characteristics of the three conceptual reactors, the ORNL blanket operates at high-temperature (1000°C), corresponding to the use of Nb-1% Zr structural material. The PPPL and UWMAK designs utilize stainless steel and correspondingly lower operating temperatures (680°C and 500°C). In the ORNL and UWMAK designs lithium is used both as the neutron moderator and coolant, while the PPPL design uses a nonconducting salt, eutectic FLIBE [(LiF)₂ BeF₂] moderator with helium coolant, thereby avoiding problems associated with the flow of conducting lithium across magnetic fields. The ORNL blanket utilizes segments with longitudinal lithium flow (parallel to B₀) except at turning sections where radial currents pump the lithium electromagnetically and reverse its flow direction. Outside the blanket regions are radiation shields which reduce the total heat load on the superconducting magnets to very small levels (1.5 to 15 kW).

The wall loading of the ORNL design is chosen sufficiently small so that the first wall and blanket structure can survive neutron radiation damage for a reactor life of ~ 20 years. In the UWMAK design, first-wall changeout is expected every two years because of radiation damage, the critical consideration being embrittlement of the stainless steel. The tritium breeding ratios are quite adequate, resulting in short (~100-day) doubling times which can well be lengthened by deliberately spoiling the breeding. The lithium inventories are of the order of 10⁶ kg, and tritium inventories are of the order of 10 kg, corresponding to T₂ concentrations of ~ 5 parts per million. This small concentration is necessary to keep the radioactive tritium loss from the plants within acceptable bounds. The tritium consumptions are typically 0.3 kg/day.

The power-balance quantities of the three conceptual power plants are as follows: The ORNL reactor is characterized by low thermal (1000 MW) and electrical powers (600 MW), corresponding to small wall loading (0.3 MW/m²) and low plasma density ($4 \times 10^{19} \text{ m}^{-3}$). However it has a large thermal conversion efficiency (56%), corresponding to its refractory metal structure and a correspondingly high operating temperature. The other two designs use stainless steel structure and more conventional steam conversion plants with correspondingly low thermal efficiencies (30 and 44%). Their thermal and electrical power outputs are much larger (5000 and 1500-to-2300 MW, respectively). The recirculating power of the PPPL (13%) design derives largely from the helium circulators, while in the ORNL design the major component is the input to the neutral-beam injectors. The UWMAK design assumes neutral-beam injection only during its 10-sec ignition phase, and it thereby makes a negligible contribution because of the 97% duty factor. The burning cycles are quite different for the PPPL and UWMAK devices, as opposed to the ORNL case.* For the assumed neoclassical diffusion

*The ORNL design used here represents a composite concept of the plasma and burn cycle of Ref. 4 adapted by the author to the "core" and power-conversion system of Ref. 5.

the confinement time is much too long for burning equilibrium, and the confinement time, τ_E , is "spoiled" to a value of 4 to 14 seconds. For the UWMAK and PPPL designs the long burn times τ_B (2000 to 6000 sec) are set by the L/R time of the plasma ring. Thus even though the PPPL and UWMAK reactors operate on long pulses they are essentially steady-state devices since $\tau_B \ll \tau_E$. They are sustained by injection of D-T ice pellets, coated with Argon impurity (40- μ m pellets at 10^6 per sec). The burning equilibria are unstable (cf. Section II) and must be servo or feedback stabilized. The burnup fraction is 7 to 12%. In the ORNL burning cycle⁵ the approach is quite different. The plasma, after ignition, is allowed to make an unstable excursion in about 20 sec to a high peak temperature (100 keV) and beta (15%), after which D-T fuel depletion (burnup fraction, 0.8) and synchrotron radiation cause a similarly sudden decrease in reaction rate, temperature (to 40 keV) and beta (5.5%). The plasma is then "driven" at an amplification factor Q between 6 and 13 by the neutral-beam injectors for about 600 sec. No confinement spoiling is used and the neutral beam injectors (30 to 60 MW at 100 to 300 A) also fuel the plasma.

In the UWMAK reactor the ohmic heating, toroidal current is excited for about 10 sec at low plasma density ($3 \times 10^{19} \text{ m}^{-3}$) with the plasma temperature leveling off at about 2 keV, after about 10 sec. In order to achieve ignition neutral beams of 350 to 500-keV D and T ions are injected tangentially to a major circumference. A total beam power input of 15 MW will cause ignition to occur in 11 sec. After ignition the temperature rises to its servo-stabilized equilibrium value of 11 keV ($T_e \approx T_i$), and the density is raised to its final value of $8 \times 10^{19} \text{ m}^{-3}$ by pellet injection. After the burn the fueling and toroidal current are decreased to cool the plasma to 500 eV, and the plasma is driven to the walls. The system is then pumped out and refueled with fresh gas. The divertors and poloidal field are then re-established. From the end of one burn to the beginning of the next is 70 sec, giving a 97% duty factor.

IV. THE THETA-PINCH REACTOR

The basic concepts of this system are shown in Fig. 11 of Ref. 1 and described in Section IV of that paper. Unlike the other magnetic confinement systems, the theta pinch is a high-beta device ($\beta \approx 1$) in which very little penetration of the magnetic field into the plasma occurs. It is characteristic of these devices in toroidal geometry that the aspect ratio is very large, of the order of 100, roughly two orders of magnitude larger than for the Tokamaks. In the theta pinch the plasma density ($\sim 10^{22} \text{ m}^{-3}$) is also two to three orders of magnitude larger than in the Mirror and Tokamak, and confinement times are correspondingly shorter. Burning times τ_B in the theta-pinch reactor are of the order of 0.1 sec rather than ~ 1000 seconds, for the Tokamak case. This relative ordering of magnitudes follows from Eq. (3) where thermonuclear power density varies as n^2 . The theta pinch is inherently a pulsed device because of its impulsive method of heating and its high instantaneous power density. For a typical cycle time $\tau_c \sim 10$ sec the duty factor $\tau_B/\tau_c \approx 10^{-3}$ results in average power

densities and wall loading which are about the same as for the other two concepts. Total toroidal magnetic energies are of the order of 100 GJ, also comparable to those of the other concepts. However, this energy is pulsed repetitively in and out of the compression-confinement coil from a superconducting magnetic energy store with risetimes of the order of 0.03 sec. This feature and the requirement of adapting the high voltage necessary for shock heating to the nuclear environment of the reactor core are essential determining factors in the design of the theta-pinch reactor.

Figure 11 of Ref. 1 shows schematically the essential elements of a staged theta-pinch reactor. In the shock-heating stage a magnetic field B_s having a risetime of the order of one μsec and a magnitude of a few T drives the implosion of a fully ionized plasma whose initial density is of the order of 10^{21} m^{-3} . After the ion energy associated with the radially-directed motion of the plasma implosion has been thermalized, the plasma assumes a temperature T_p , characteristic of collisional equilibration of the ions and electrons (Ref. 1, Fig. 11). After a few hundred μsec the adiabatic compression field is applied by energizing the compression coil. The plasma is compressed to a smaller radius and its temperature is raised to a value at or near ignition ($\sim 5 \text{ keV}$). As the D-T plasma burns for several tens of msec, it produces 3.5-MeV α particles which partially thermalize with the electrons and the D-T ions as the burned fraction of plasma increases to a few percent. As a result the plasma is further heated. Since β is approximately unity, and since B is approximately constant, the plasma expands against the magnetic field (not shown in Ref. 1, Fig. 11), doing work ΔW which is about 62% of the thermonuclear energy deposited by α particles. This work produces an emf which forces magnetic energy out of the compression coil and back into the compression magnetic-energy store. This high- β , α -particle heating and the resulting direct conversion are important factors in the overall reactor power balance.

A cross section of the reactor core is shown in Fig. 7. The first wall is composed of the ends of insulator-coated blanket segments in which lithium is used both as a moderator and a coolant. The insulator must be thin enough to allow heat extraction from the plasma Bremsstrahlung and nuclear radiation, as well as to allow passage of heat from the plasma as it is being quenched at the end of a burning pulse. Simultaneously the insulator must support the back-emf electric field E_θ of the plasma implosion during the fraction of a microsecond of shock heating. During this short time of high-voltage stress there is no radiation present, as there is later during the burn. Hence the insulator requirement of a resistivity of $\sim 10^8 \Omega \cdot \text{m}$ and a dielectric strength $E_D \sim 10^7 \text{ V/m}$ at a temperature in the neighborhood of 1000°C need not be met in the presence of a high radiation field. Allowing N blanket segments each coated with an insulator of thickness X_D to support a total voltage of $2\pi b E_\theta$, we find $N = \pi b E_\theta / X_D E_D$. Heat transfer calculations show that $X_D = 3 \times 10^{-4} \text{ m}$ is adequately thin, corresponding to $N = 100$ blanket segments. With niobium metal structure as shown in Fig. 7 it is found that the blanket provides a tritium breeding ratio of 1.11 and an energy multiplication

such that $ME_n = 20.5 \text{ MeV}$, while adequately protecting the room-temperature copper compression coil from nuclear radiation.

The implosion-heating coil of Fig. 7 is of an end-fed design in which the field B_s is admitted to the plasma region between the blanket segments, being excluded from them by the skin effect during shock-heating times and later penetrating the segments during the time of electron-ion equilibration.

The compression coil has sufficient thickness (low-current density) that joule losses of the theta currents which produce the compression field B_0 are reduced to such a level that their contribution to the plant circulating power is acceptable. The coil is layered in $\sim 2\text{-mm}$ thicknesses to reduce to negligible proportions the eddy-current losses during the 0.03-sec rise and fall of the compression field.

Similarly the segmenting of the blanket provides negligible eddy-current losses in the lithium and graphite. An overall view of the conceptual RTPR power plant is shown in Fig. 8. The reactor ring

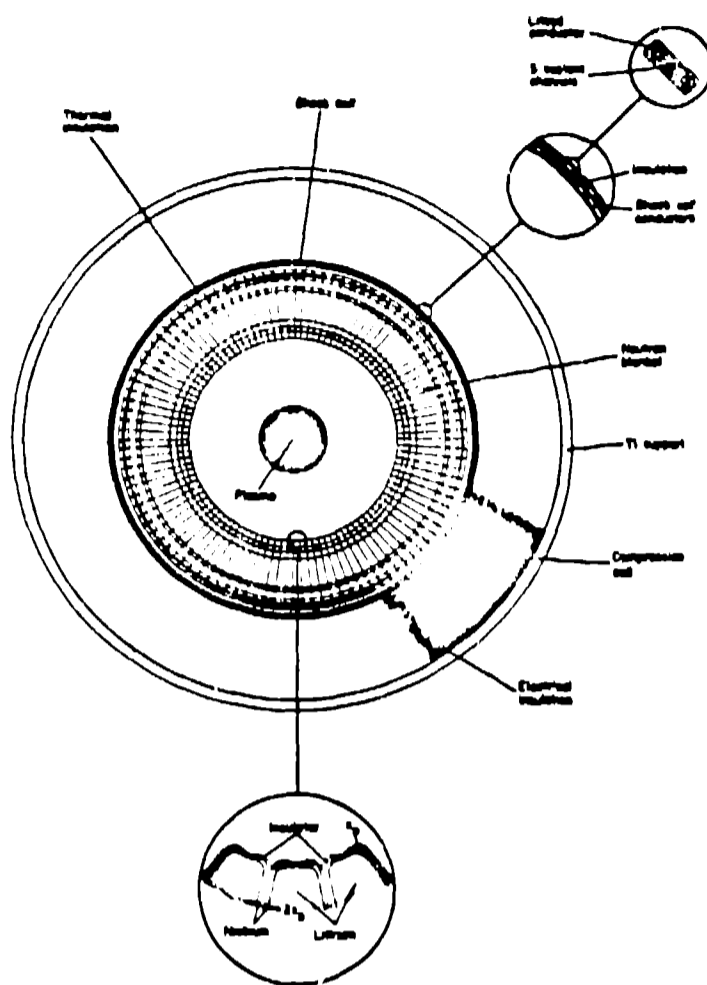


Fig. 7. Cross section of the neutron blanket, shock-heating coil and adiabatic compression coil of the Reference Theta-Pinch Reactor.

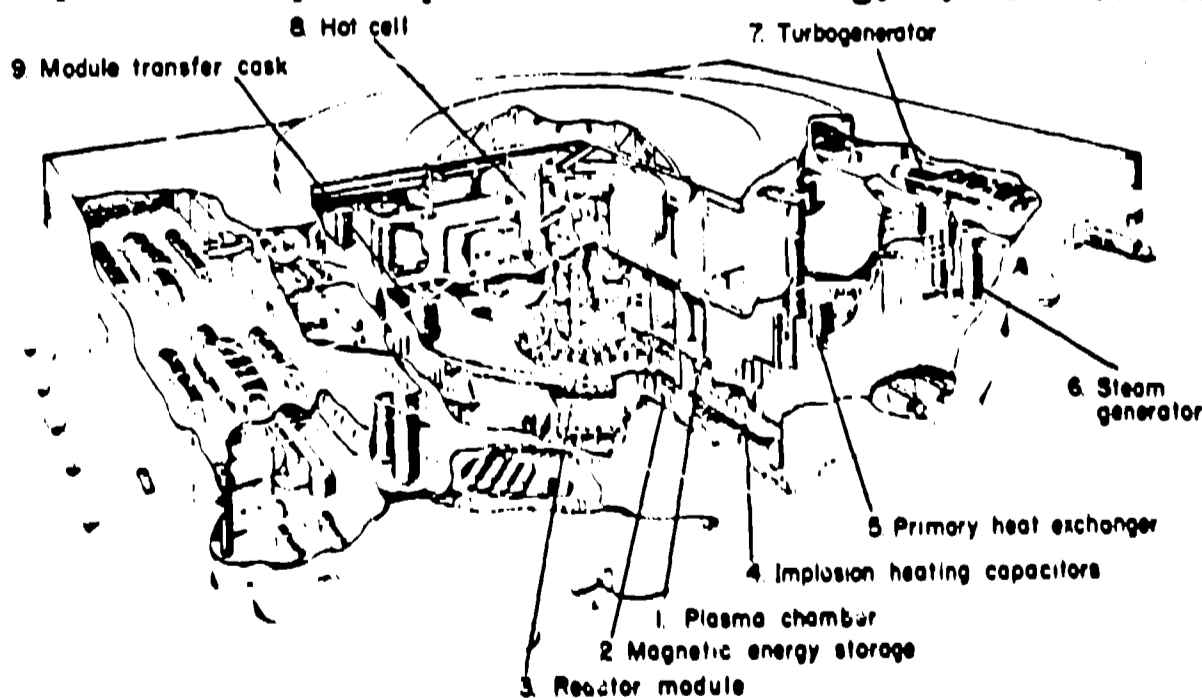


Fig. 8. Overall view of the LASL-ANL θ -pinch fusion power plant.

is below ground in an evacuated tunnel with a helium barrier to prevent escape of tritium. The transfer cask allows removal of the radioactive core modules for replacement in case of failure. During the burn cycle direct-conversion work of 9.8 MJ per meter of reactor length is produced, as compared with a thermonuclear energy $W_N = 93$ MJ/m. The ratio of direct-conversion energy to thermally-converted electrical energy is $\Delta W/\eta_T W_N = 0.26$ for $\eta_T = 0.40$.

An attractive feature of a pulsed fusion reactor is the possibility of removing the alpha-particle "ash" resulting from the burnup of the deuterium-tritium fuel mixture and injecting fresh fuel between burning pulses. No divertor is required, as in the case of a steady-state, toroidal reactor. A layer of neutral gas injected between the hot central plasma and the first wall is used to cool, neutralize, and purge the partially burned D-T plasma. Preliminary calculations show that sputtering problems are alleviated because heat transfer to the wall, which would otherwise occur by energetic ions, will now occur primarily by means of low-energy neutral atoms and to a lesser extent by ultraviolet and visible radiation.

Table II provides a summary of the theta-pinch reactor plasma and magnetic-field parameters. The tritium inventory, breeding ratio and doubling time are comparable to those of the Tokamak reactors. The wall loading is about 40% higher than for the PPPL and UWMAK reactors. The toroidal magnetic energy is less for the RTPR by a factor of two to three, but, owing to its pulsed character, it should be compared to the poloidal magnetic energy of UWMAK. It is twice as large and rises

TABLE II Plasma and magnetic-field parameters for the LASL-ANL conceptual Theta-Pinch reactor.

Plasma:

Beta	0.8 - 1.0
Major Radius R, m	56
Plasma Radius a: Shock, Burn, m	0.38, 0.12
Plasma Aspect Ratio A, max	465

Magnetic Fields:

Shock, Comp. Coil Radii, m	0.91, 0.94
Shock Field, T	1.4
Compr., Burn Field, T	11.0
Helical Poloidal Field, T	0.8
Compr. Field Risetime, sec	0.031
Supercond. Mag. Energy, GJ	102
Shock-Heating Energy, GJ	0.9

much faster. The plasma burn quantities are quite different than those of the Tokamaks, with exception of the $n\tau$ and fuel-burnup parameters which are comparable.

In the power balance we have power output (2000 MWE), circulating power fraction ($E = 13\%$), and Q value (14) comparable to those of the Tokamak systems. A unique feature of the Theta Pinch is the direct conversion power, discussed above, which offsets the compression-coil joule losses to provide the relatively low circulating power and high plant efficiency. The power level of the RTPR is inversely proportional to the cycle time τ_c since the essential plasma operation and energy balance are determined for a given pulse. The choice $\tau_c = 10$ sec gives low wall loading and long first-wall lifetime, rather than optimum economy, which would be more favorable at the shortest cycle time allowed ($\tau_c \approx 3$ sec).

V. THE MAGNETIC-MIRROR REACTOR

The basic concepts of the Magnetic Mirror are shown in Figs. 3 and 18 of Ref. 1 and described in Section V of that report. Here, however, we point out the LLL choice of the Yin-Yang coil geometry¹¹, rather than the Baseball geometry, for providing the minimum-B magnetic field. The Yin-Yang coil of the LLL reactor design is shown in Fig. 11.

The toroidal reactors described in the previous sections allow the possibility, under ideal confinement conditions, of plasma ignition, i.e., the plasma can be self-sustaining, requiring little or no injected energy. Under these conditions the amplification factor Q Eq. (12) of the plasma itself becomes very large. The magnetic-mirror, because it is an open-ended device with an intrinsic loss of plasma, allows no such operation. Under ideal collisional circumstances the theoretical value of Q is only slightly greater than unity (about 1.2 for the mirror ratios considered here). The magnetic-mirror plasma is therefore a driven power amplifier whose power output is a factor Q times its injected power. In order to achieve economical net output with such low values of Q a magnetic-mirror reactor must make use of the plasma energy which escapes from its mirror in order to power the injectors. The means by which this is accomplished at high efficiency is called direct conversion. This leads to a large recirculating power fraction, of order unity. However, the power circulation loop does not pass through the thermal-conversion equipment and can be shown to be economical if its efficiency is sufficiently high.

The method by which the injection power is supplied directly from the energy of plasma ions which escape out the mirrors is illustrated in Fig. 9. The fraction $(1-h) P_N$ of thermonuclear power which occurs as α particles remains in the plasma and, along with $\eta_I P_I$, is converted to useful electrical output through a direct converter of efficiency η_D . The thermal converter provides useful output and that recirculating power necessary to sustain itself. According to Fig. 9 net power output occurs when

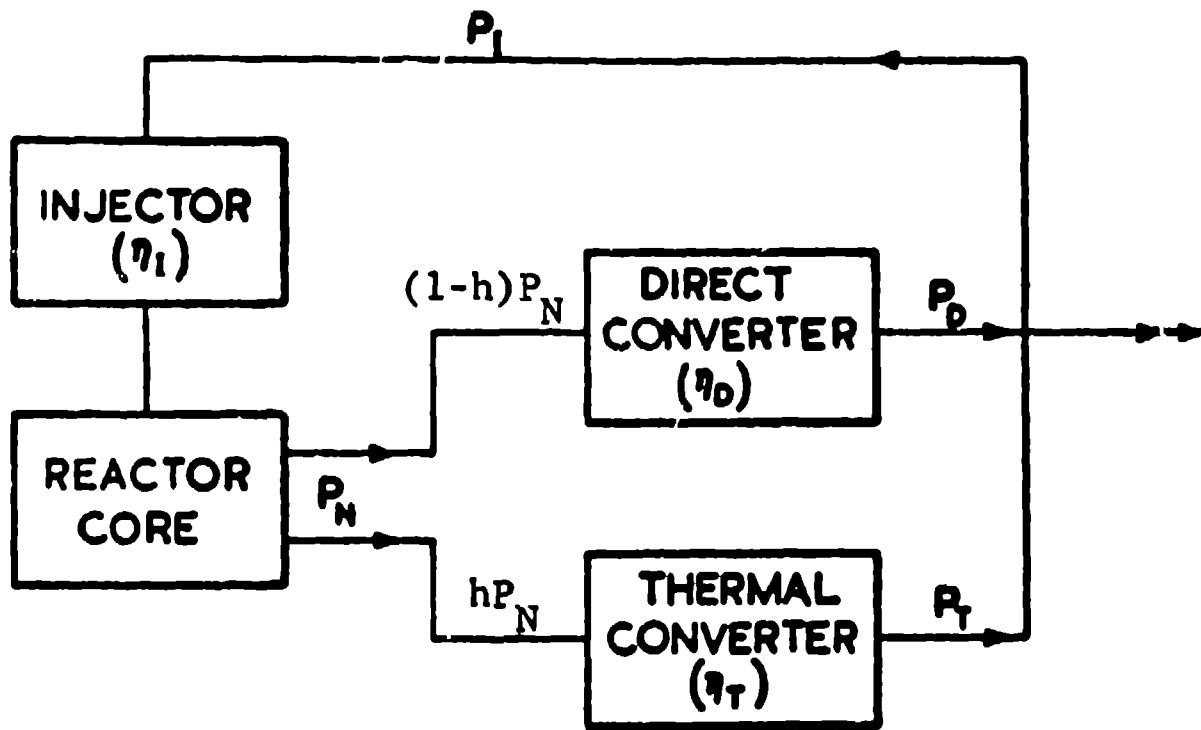


Fig. 9. Power flow diagram showing the main features of a Magnetic-Mirror power plant with direct conversion.

$$\eta_T h P_N + \eta_D [(1-h) P_N + \eta_I P_I] - P_I > 0. \quad (20)$$

Using $Q = P_N / \eta_I P_I$, this corresponds to the condition

$$Q > \frac{1 - \eta_D \eta_I}{\eta_I [h \eta_T + (1-h) \eta_D]}. \quad (21)$$

R. F. Port and his colleagues have shown that values of η_D as large as 0.8 can be attained. For $\eta_T = 0.8$, inequality (21) shows that reactor breakeven can occur for Q values as low as 0.8, thus allowing the system to accommodate the attainable value of about 1.2.

The method by which end-loss plasma energy from a magnetic mirror is converted to useful electrical power is illustrated in Fig. 10. This shows a vertical section of one mirror of a minimum-B mirror system like that of Fig. 11 and a typical escaping ion orbit. First the escaping plasma is expanded in the horizontal fan-shaped magnetic field which extends 75 m from the mirror. In this process the plasma density is reduced, and the ion motion is converted, by means of an inverse of the mirroring process, into motion parallel to the field lines. After expansion, the plasma density is sufficiently low ($\sim 10^{13}$ ions/m³) that charge separation of ions and electrons can occur. The electrons (whose energy is negligible) are diverted away vertically in the separator along the magnetic lines, but the ions escape across the lines and continue horizontally to a collector. Here, depending on their energy, the ions are decelerated in a periodic set of charge-collecting electrodes which collect them as they are brought to rest by the retarding potentials. There results a distribution of high voltages on the collector electrodes which store the energy of the slowed-down

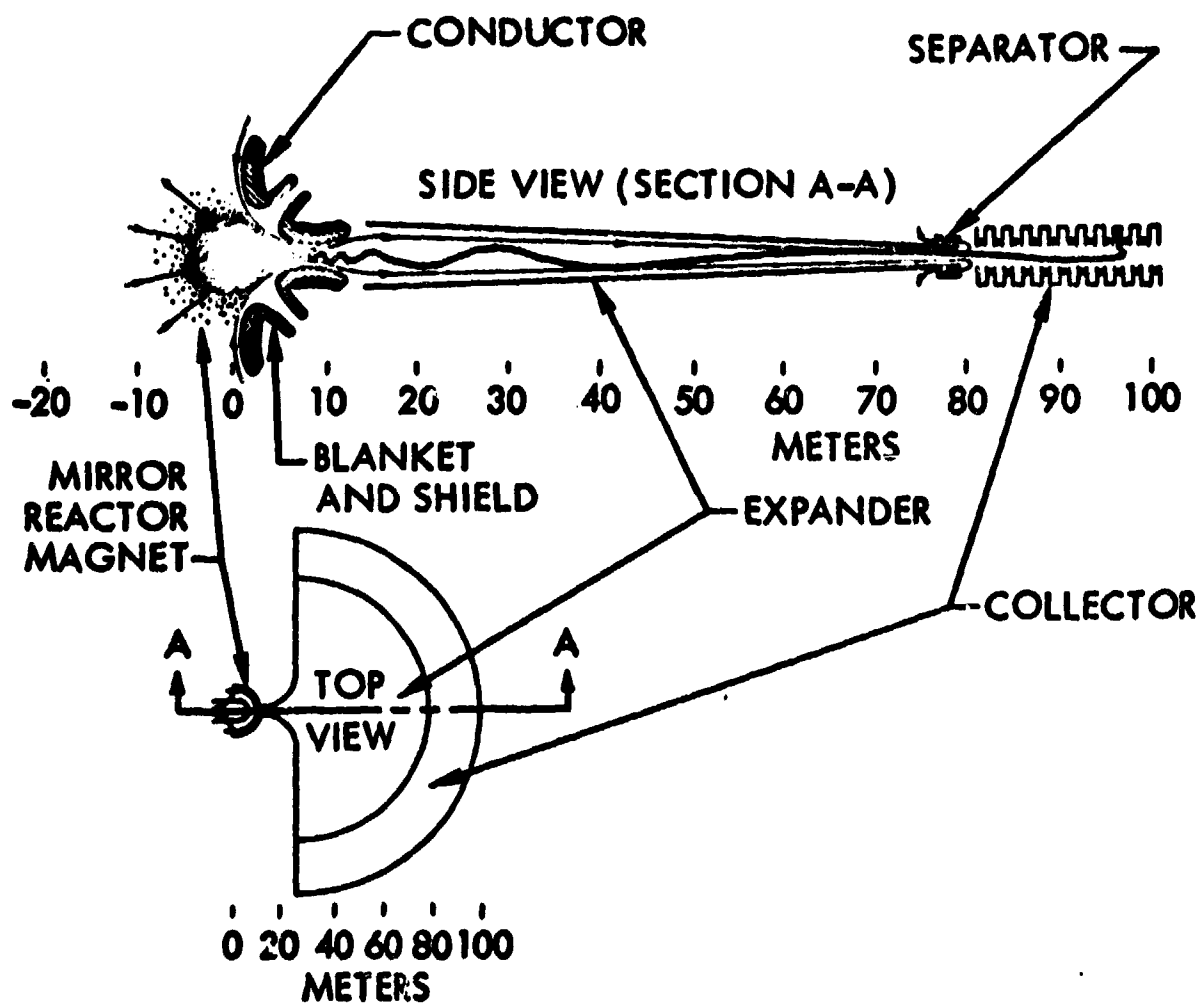


Fig. 10. Illustrating the main components of an apparatus for converter end-loss ion energy from a mirror reactor into direct-current electrical output.

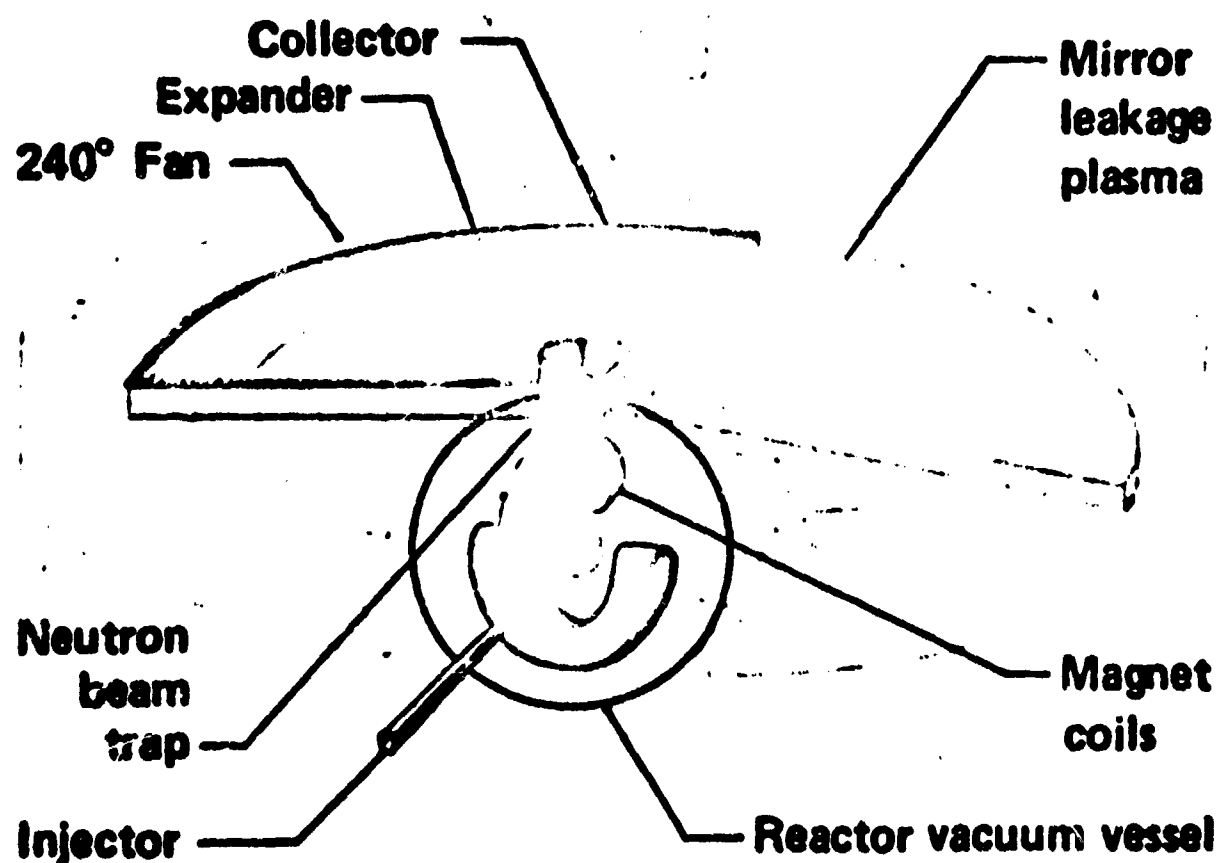


Fig. 11. Illustrating the main components of the LLL Magnetic-Mirror Reactor with direct conversion.

ions. These voltages are then brought to a common D.C. potential V_D and used to power the neutral-beam injectors.

The main features of the LLL Magnetic-Mirror Reactor are summarized in Table III. A schematic view of the power plant is shown in Fig. 11. The central plasma core is a nearly spherical ellipsoid of about 3.3-m mean radius, injected by 490 MW of neutral beam at an average ion energy of 550 keV and a current of 890 A over a total area of 5 m². The mean plasma ion energy is 620 keV; its density is 1.2×10^{16} m⁻³; and its β is 0.85.

The Yin-Yang coils have a mean radius in their "fan" planes of 10 m, a winding width of 6.6 m and a distance of 4.2 m between the parallel semicircular sides. All of the coil conductor is protected from neutron radiation by a 1-m-thick lithium blanket and shield, arranged so that the lithium flow is predominantly (90%) along magnetic lines. The coils are designed to produce a central field of 5 T and a maximum field in the fans of 15 T, (16.5 T on the superconductor) corresponding to a vacuum mirror ratio $R_V = 3.0$ and an effective ratio due to plasma diamagnetism $R_{eff} = R_V / (1 - \beta)^{1/2} = 7.7$. The escaping plasma beam has an area of 1.5 m², produced by weakening the mirror field on one side over this limited area.

TABLE III Plasma and magnetic field parameters of the LLL 200 MWe DT Mirror Reactor

Plasma:

Shape	Ellipsoidal, Min. B, Vol.
Beta	0.85
Mean Ion Energy, MeV	0.62
Z Axis Intercept, m	3.5
Volume m ³	130
Density m ⁻³	1.2×10^{20}
Beam Area at Mirror, m ²	1.5

Magnet Coil:

Radius, m	10
Width of Coil, m	6.6
Coil Separation, 2h, m	4.2
Central Field, T	5
Mirror Field, T	15
Mirror Ratio, Vac.	3
Mirror Ratio, $\beta = 0.85$	7.7

The plasma beam escaping from the vertical mirror of Fig. 11 into the expander is first deflected by 90 degrees along the mirror magnetic lines which are bent by means of "steering" coils. The neutrons emerging from the mirror are buried in a neutron trap. From the mirror to the end of the expander the magnetic field decreases from 15 T to 0.15 T, decreasing the perpendicular ion energy by a factor of 100.

The expander has a horizontal radial extent of 76 m, accepting a beam height of 0.87 m over a total horizontal angle of 240° . Past the expander the electrons are deflected away by separator coils, and the ion energy is converted over the 22-m radial length of the collector. The expander and collector are enclosed in a containment vessel of three radial sections separated by 1.7 m, composed of dished hexagonal modules, each with a horizontal dimension of about 32 m. Support columns intercept about 3% of the plasma beam. In addition to this flat containment vessel there is a spherical vacuum vessel, mostly below ground level, in order to limit tritium leakage to the atmosphere.

The thermonuclear power carried by neutrons is 470 MW, and the escaping power of charged particles is 610 MW. Emerging from the direct converter ($\eta_D = 0.70$) are 430 MW and from the blanket and thermal conductor ($\eta_T = 0.45$) are 360 MW. Accounting for 560 MW of injection energy and 20 MW to auxiliaries, the net electrical output is 170 MW, giving an overall efficiency of 27%. The system Q is chosen to be 1.2.

REFERENCES

1. H. P. Furth, Magnetic Confinement of Thermonuclear Plasmas, Bull. Am. Phys. Soc., Ser. II, 19, No. 1, 85 (1974). Preceding paper of these proceedings.
2. Proceedings, British Nuclear Energy Society Nuclear Fusion Reactor Conference, September, 1969. (UKAEA, Culham Laboratory, Abingdon, Berks., 1970).
3. R. G. Mills, et al., in Proceedings of the Texas Symposium on Controlled Thermonuclear Experiments and Engineering Aspects of Fusion Reactors, November 20-22, 1972, Paper II/B.6. Also private communication (1973).
4. A. P. Fraas, Oak Ridge National Laboratory Report, ORNL-TM-3096 (May 1973).
5. J. F. Etzweiler, J. F. Clarke, and R. H. Fowler, Oak Ridge National Laboratory Report ORNL-TM-4083 (June, 1973).
6. B. Badger, et al., Wisconsin Tokamak Reactor Design, University of Wisconsin Nuclear Engineering Department Report UWFD-68 (November, 1973) Vol. 1.
7. R. A. Krakowski, et al., Joint Los Alamos Scientific Laboratory and Argonne National Laboratory Report, LA-5336/ANL-6019 (December 1973).
8. R. W. Werner, et al., in Proceedings of the Texas Symposium on Controlled Thermonuclear Experiments and Engineering Aspects of

Fusion Reactors, November 20-22, 1972. Paper 1, Session IV.
Also private communication (1973).

9. D. R. Sweetman, Nuclear Fusion 13, 157 (1973).
10. R. G. Mills, Proceedings, British Nuclear Energy Society Nuclear Fusion Reactor Conference, September 1969. (UKAEA, Culham Laboratory, Abingdon, Berkshire, 1970). p. 322.
11. R. W. Moir and R. F. Post, Nuclear Fusion 9, 253 (1969).